

# Magneto-Thermo-Mechanical Analysis of Electromagnetic Devices Using the Finite Element Method

Michael G. Pantelyat

**Abstract**—Fundamental basics of pure and applied research in the area of magneto-thermo-mechanical numerical analysis and design of innovative electromagnetic devices (modern induction heaters, novel thermoelastic actuators, rotating electrical machines, induction cookers, electrophysical devices) are elaborated. Thus, mathematical models of magneto-thermo-mechanical processes in electromagnetic devices taking into account main interactions of interrelated phenomena are developed. In addition, graphical representation of coupled (multiphysics) phenomena under consideration is proposed. Besides, numerical techniques for nonlinear problems solution are developed. On this base, effective numerical algorithms for solution of actual problems of practical interest are proposed, validated and implemented in applied 2D and 3D computer codes developed. Many applied problems of practical interest regarding modern electrical engineering devices are numerically solved. Investigations of the influences of various interrelated physical phenomena (temperature dependences of material properties, thermal radiation, conditions of convective heat transfer, contact phenomena, etc.) on the accuracy of the electromagnetic, thermal and structural analyses are conducted. Important practical recommendations on the choice of rational structures, materials and operation modes of electromagnetic devices under consideration are proposed and implemented in industry.

**Keywords**—Electromagnetic devices, multiphysics, numerical analysis, simulation and design.

## I. INTRODUCTION

THIS paper deals with mathematical models, numerical techniques and scientific software for 2D and 3D coupled magneto-thermo-mechanical analysis of various electromagnetic and electromechanical devices: Modern induction heaters, household induction cookers, and rotating electrical machines (mainly large synchronous turbogenerators). The development of numerical methods and tools for the computer simulation of modern electrical and electromechanical devices and technological processes is an important problem in science and engineering. From pure scientific and engineering viewpoints, it is extremely important to have a possibility to determine rational operating and structural conditions of the above devices by means of relatively cheap computer simulation without utilization of expensive full-scale experiments. The results of computations allow recommending such operational, technological and structural parameters as operation voltages or currents,

M.G. Pantelyat is with the Department for Electrical Apparatus, National Technical University "Kharkiv Polytechnic Institute", Kharkiv, UA-61002 Ukraine (e-mail: m150462@yahoo.com).

frequency of electromagnetic oscillations, durations of heating and cooling, type and parameters of cooling media, arrangements of inductors or field coils, air gaps, physical properties of materials to be used, etc.

Development of mathematical models, numerical algorithms and applied software for computer simulation of the electromagnetic devices are carried out by taking into consideration coupled character of the magnetic, thermal and mechanical processes during their operation (see Fig. 1) [1]. The presence of the electromagnetic field produces thermal and mechanical phenomena. Eddy current losses alter the temperature distribution and lead to the heating of the device under consideration or its separate structural parts. The temperature gradients and electromagnetic forces alter the mechanical state of the structure and cause its elastic or plastic mechanical deformations. Furthermore, the non-stationary temperature field influences the electromagnetic field distribution because the electrophysical material properties (electrical conductivity and/or magnetic permeability) of metallic structural parts depend on temperature. Besides, to obtain precise numerical results, it is important to take into account temperature dependencies of thermal and mechanical material properties. All these effects influence the operational and/or technological conditions of the device. From engineering point of view, knowledge of magneto-thermo-structural state of electrical and electromechanical devices is required to avoid possible operational or technological difficulties and to recommend appropriate parameters of devices under consideration.

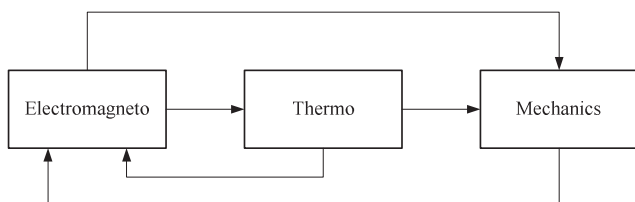


Fig. 1 Relations among the processes under consideration

The paper presents mathematical models and numerical techniques for finite element analysis of coupled nonlinear magneto-thermo-mechanical problems regarding various types of modern electrical engineering devices and technologies. Peculiarities of numerical simulations of coupled multiphysical phenomena regarding various types of electrical and electromechanical devices under consideration are

described in details. Numerical results describing solution of real problems of practical interest are presented and analyzed. The problems are solved in 2D and 3D formulations by the finite element method using in-house scientific computer codes written in C language.

## II. MATHEMATICAL MODELS

The processes in the above-mentioned devices generally represent complex multiphysics phenomena. Their mathematical models usually consist of two or three non-linear and non-stationary partial differential equations (PDEs) describing the above fields, whose coefficients given by material parameters may depend on the state variables (mostly the temperature).

In this section, the mathematical models in 3D formulations are presented. 2D mathematical models are obtained from 3D ones using necessary simplifications.

### A. Electromagnetic Fields

The governing equations for the description of 3D transient low-frequency electromagnetic fields (on the order of 10–10<sup>5</sup> Hz) with the Coulomb gauge using magnetic vector potential  $\mathbf{A}$  and electric scalar potential  $\varphi$  can be formulated as [2]:

$$\operatorname{curl}\left(\frac{1}{\mu} \operatorname{curl} \mathbf{A}\right) - \operatorname{grad}\left(\frac{1}{\mu} \operatorname{div} \mathbf{A}\right) + \gamma\left(\frac{\partial \mathbf{A}}{\partial t} - \mathbf{v} \times \operatorname{curl} \mathbf{A} + \operatorname{grad} \varphi\right) = \mathbf{J}_{\text{ext}}, \quad (1)$$

$$\operatorname{div}\left(\gamma\left(\frac{\partial \mathbf{A}}{\partial t} - \mathbf{v} \times \operatorname{curl} \mathbf{A} + \operatorname{grad} \varphi\right)\right) = 0. \quad (2)$$

where  $\gamma$  is the electrical conductivity of the material,  $\mu$  denotes the magnetic permeability,  $\mathbf{v}$  stands for the velocity and  $\mathbf{J}_{\text{ext}}$  is the field current density.

The field distribution is then used to calculate the Joule and magnetization losses and force or torque effect.

### B. Temperature Field

The temperature field distribution in systems with motion is generally described by the transient heat transfer equation [3] in the form

$$\operatorname{div}(\lambda \cdot \operatorname{grad} T) = \rho c \left( \frac{\partial T}{\partial t} + \mathbf{v} \cdot \operatorname{grad} T \right) - Q, \quad (3)$$

where  $\lambda$  is the thermal conductivity,  $\rho$  denotes the mass density,  $c$  is the specific heat, and symbol  $Q$  represents the given internal volumetric heat sources. Numerous physical parameters of the materials are also nonlinear functions of the temperature.

A considerable role is here played by the boundary conditions of convection and radiation; particularly important is to correctly determine the coefficients of convection, emissivity, configuration factors, factors of multiple reflections, etc.

### C. Mechanical State of Devices

Elastic-plastic mechanical status of structural parts of the considered devices is described by the following system of three-dimensional tensor equations [4]:

$$\begin{aligned} \sigma_{ij,i} + f_j &= 0, \\ \varepsilon_{ij} &= \frac{1}{2}(u_{i,j} + u_{j,i}), \\ \sigma_{ij} &= \frac{E}{1+\nu}(\varepsilon_{ij} + \frac{\nu}{1-2\nu}\delta_{ij}e), \end{aligned} \quad (4)$$

where  $\boldsymbol{\sigma}_{ij}$  is the tensor of the mechanical stresses,  $\boldsymbol{\varepsilon}_{ij}$  is the tensor of mechanical strains,  $\mathbf{u}_{ij}$  is the vector of mechanical displacements,  $\mathbf{f}_i$  is the vector of the external volumetric forces,  $E$  is the temperature-dependent modulus of elasticity of the material,  $\nu$  is the temperature-dependent Poisson ratio of the material,  $\delta_{ij}$  is the Kronecker delta function, and  $e = \varepsilon_{kk}$ .

The first part of (4) is the system of equilibrium equations describing the correlation between the mechanical stress tensor

$$\sigma_{ij} = \begin{pmatrix} \sigma_{11} & \sigma_{21} & \sigma_{31} \\ \sigma_{12} & \sigma_{22} & \sigma_{32} \\ \sigma_{13} & \sigma_{23} & \sigma_{33} \end{pmatrix} \quad (5)$$

and given volumetric forces components  $f_i$ .

The second part of (4) is the system of kinematic equations representing the correlation between the strain tensor

$$\varepsilon_{ij} = \begin{pmatrix} \varepsilon_{11} & \varepsilon_{21} & \varepsilon_{31} \\ \varepsilon_{12} & \varepsilon_{22} & \varepsilon_{32} \\ \varepsilon_{13} & \varepsilon_{23} & \varepsilon_{33} \end{pmatrix} \quad (6)$$

and components  $u_i$  of the mechanical displacement vector.

The third part of (4) is the constitutive equations presenting the correlation between the mechanical stress tensor  $\boldsymbol{\sigma}_{ij}$  and strain tensor  $\boldsymbol{\varepsilon}_{ij}$ .

The axisymmetric mechanical deformed state of the device is described by the system of equations [4]

$$\begin{aligned} \frac{\partial \sigma_{rr}}{\partial r} + \frac{\partial \tau_{rz}}{\partial z} - \frac{\sigma_{rr} - \sigma_{\theta\theta}}{r} + F_r &= 0; \\ \frac{\partial \tau_{rz}}{\partial r} + \frac{\partial \sigma_{zz}}{\partial z} + \frac{\tau_{rz}}{r} + F_z &= 0; \\ \varepsilon_{rr} &= \frac{\partial u_r}{\partial r}; \quad \varepsilon_{zz} = \frac{\partial u_z}{\partial z}; \\ \gamma_{rz} &= \frac{\partial u_r}{\partial z} + \frac{\partial u_z}{\partial r}; \quad \varepsilon_{\theta\theta} = \frac{u_r}{r}, \end{aligned} \quad (7)$$

where [4]  $\sigma_{rr}$ ,  $\sigma_{zz}$ ,  $\sigma_{\theta\theta}$ ,  $\tau_{rz}$  are the radial, axial, circumferential and shear mechanical stresses, respectively,

$\varepsilon_{rr}$ ,  $\varepsilon_{zz}$ ,  $\varepsilon_{\theta\theta}$ ,  $\gamma_{rz}$  are the radial, axial, azimuthal and tangential mechanical strains, respectively,  $u_r$  and  $u_z$  are the radial and axial mechanical displacements, and  $F_r$ ,  $F_z$  are the given radial and axial forces, respectively.

In order to simulate the mechanical state of the structure under consideration, elastic, plastic and thermal deformations are considered [5].

The static elastic-plastic mechanical problem is solved using the finite element method [5]. Mechanical displacements are calculated at the nodes of the finite elements. Deformations and mechanical stresses are determined in the centers of the finite elements because there they exhibit the maximum accuracy [5].

A detailed description of the numerical technique used to solve elastic-plastic mechanical problems can be found in [5].

### III. NONLINEAR MATERIAL PROPERTIES

When solving coupled problems in electrical and electromechanical devices, it is necessary to take into account that equations describing transient electromagnetic, thermal and mechanical phenomena are essentially nonlinear because all material parameters depend on the temperature. Moreover, the magnetic permeability of ferromagnetic materials depends on the magnetic flux density. For example, Figs. 2–6 show some characteristics of typical ferromagnetic carbon steel CSN 12 040 [6].

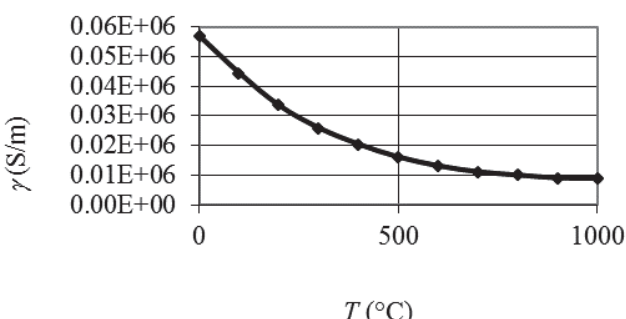


Fig. 2 Temperature dependence of electrical conductivity for carbon steel 12 040

To calculate the values of electrical, thermal and mechanical material properties (thermal conductivity, specific heat, modulus of elasticity, etc.) for intermediate temperatures, several more or less sophisticated ways can be used. The simplest one is a piecewise linear approximation, more sophisticated are approximations based on polynomials of higher orders (for example splines).

For numerical computation of nonlinear electromagnetic fields, it is necessary to select an effective method for approximation of the magnetization curve  $B - H$  and dependence  $\mu_r(B)$  describing the magnetic properties of soft ferromagnetic materials (see Fig. 5). These curves may significantly differ in the dependence on the content of various levels in the considered steel. Their modeling can be best

realized by means of the cubic splines, which is for this specific case (steeply changing values of  $\mu_r$  in the vicinity of the knee) probably the most versatile and reliable method.

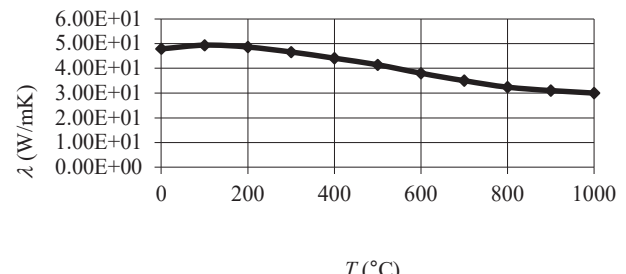


Fig. 3 Temperature dependence of thermal conductivity for carbon steel 12 040

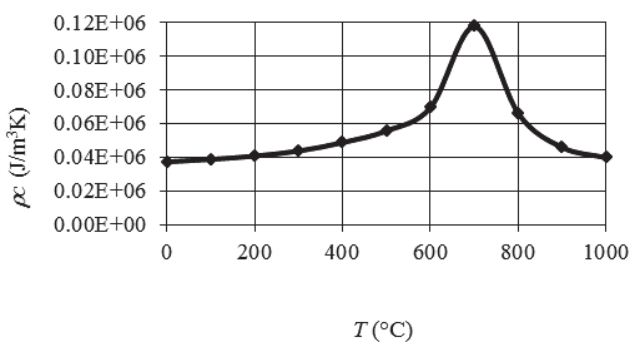


Fig. 4 Temperature dependence of specific heat capacity for carbon steel 12 040

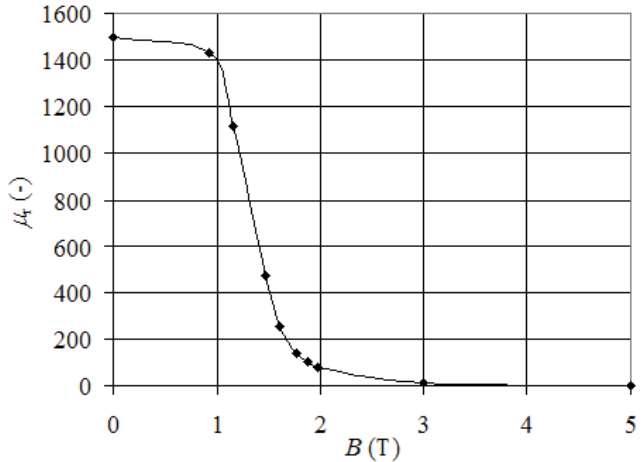


Fig. 5 Dependence  $\mu_r(B)$  for carbon steel 12 040 for  $T = 20^\circ\text{C}$

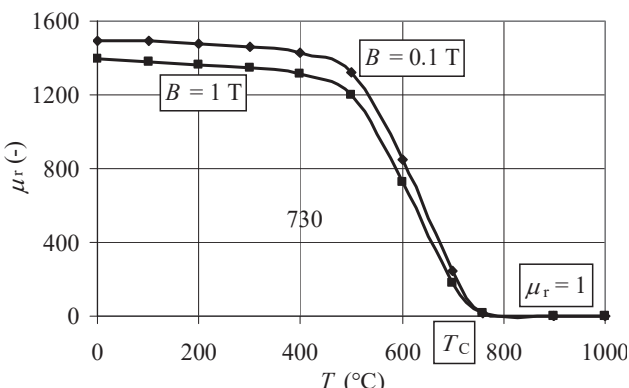


Fig. 6 Dependencies  $\mu_r(T)$  for carbon steel 12 040 for two different values of magnetic flux density  $B$

In some industrial applications of electromagnetic fields (induction heating of metal workpieces, etc.) the temperature of treated parts reaches very high values (800–1100 °C and even more depending on the type of the technological process). In such a case it is important to take into account the temperature dependence of magnetic permeability of soft ferromagnetic materials [7] (see Fig. 6). The dependencies depicted in Fig. 6 have three main parts:

- At relatively “low” temperatures (up to 500–550 °C, approximately) magnetic permeability  $\mu_r$  of soft ferromagnetic materials practically does not depend on temperature,
- With increasing temperature, the magnetic permeability decreases very fast,
- When the temperature reaches the so-called Curie point  $T_C$ , the soft ferromagnetic material loses its magnetic properties and becomes non-magnetic ( $\mu_r=1$ ). For structural steels the value of  $T_C$  is about 760–770 °C (see [7]).

To compute distributions of nonlinear electromagnetic fields in high-temperature devices it is necessary to select suitable methods for approximation of the temperature dependence of magnetic permeability of soft ferromagnetic materials and recommend effective approaches for practical utilization.

Detailed analysis carried out by the author is shown in [7]. They proved that the analytical dependences cannot effectively be used for approximation of the magnetic properties of soft ferromagnetic materials. As mentioned above, one of the possible ways is using the linear interpolation between two neighboring measured values or the method of splines. On the other hand, the temperature dependence  $\mu(T)$  of the magnetic permeability of soft ferromagnetic materials can relatively easily be described by an analytical function. Typical is the approximation presented in [7].

#### IV. NUMERICAL MODELLING OF COUPLED (MULTIPHYSICAL) MAGNETO-THERMO-MECHANICAL PROCESSES

In order to develop accurate and reliable mathematical models, numerical algorithms, and software for numerical analysis of the mentioned devices, we must take into consideration the coupled character of the electromagnetic, thermal and mechanical processes taking place in their structural parts (see Fig. 1). During their operation the electromagnetic field causes thermal and mechanical phenomena [1]. Eddy current losses alter the temperature distribution and lead to the heating of structural parts of devices under consideration. The temperature gradient and electromagnetic forces alter the mechanical state of the structures and cause their reversible elastic or irreversible plastic mechanical deformations. In the general case, the non-stationary temperature field in its turn influences the electromagnetic field distribution because the conductivity and permeability of materials depend on the temperature. Besides, it is important to take into account the temperature dependencies of thermal and mechanical properties of the involved materials. We will show it on two cases of simulation:

##### A. Devices with High Temperatures of Structural Parts

Examples are fast high-temperature induction heating devices with final temperature of 800–1000 °C and even more for example induction heaters for large steel disks treatment [8] (temperature more than 1100 °C), etc. During their numerical analysis it is necessary to pay special attention to the temperature dependencies of all material constants (see Figs. 2–4, 6). In order to satisfy this demand, it is necessary to simulate distributions of electromagnetic and thermal fields iteratively (see Fig. 1). This is an example of so-called indirect or weak coupling [9]. Weakly coupled problems are solved [9] using cascade algorithms. The coupled fields are solved in successive steps. The coupling is performed by applying results from the first analysis (involving only electromagnetic field simulation) as the inputs for the second analysis (which involves the temperature field computation). Thus, the problem is divided into several subproblems and solved sequentially in an iteration loop until it converges. After reaching the corresponding criterion it is possible to compute mechanical state of the structural parts of the device. Such a method can be used for numerical analysis of some structural parts of a turbogenerator (for example, rotor slot wedges depicted in Figs. 7, 8) where local temperature during transient unbalanced operation can reach 400 °C [10].

##### B. Devices with Relatively Low Temperatures

We can mention household induction cookers [11] with maximum temperatures about 200 °C, end regions of turbogenerators [12] (working temperature does not exceed 105–110 °C), etc. In such devices higher temperatures are unacceptable due to possible damage or destruction of some insulating elements. In this situation the electromagnetic field can be solved independently of the other fields (temperature field and field of mechanical strains and stresses), without

respecting the dependence of electrical conductivity and magnetic permeability on temperature. This simplification can be accepted practically without any negative influence on the results because of rather lower temperature rise. As for the thermal and stress-strain states, they must usually be solved as hard coupled. The solution is obtained in turn at each time step starting from the knowledge of distribution of the internal sources of heat. Even when the mechanical problem is considered linear (without plastic deformations), searching of the unknown contact domain (or domains) between both parts in each step is realized by means of an iterative process [6].

## V. NUMERICAL RESULTS

### A. Heating of a Turbogenerator Rotor

The developed numerical technique is used to calculate the transient temperature distribution in the rotor of a large turbogenerator at a line-to-line short circuit characterized by the travelling wave of negative sequence current density (100 Hz) in the stator. Design and a simplified model of a 300 MVA class turbogenerator rotor (its end zones are not considered) are presented in Figs. 7, 8, respectively.

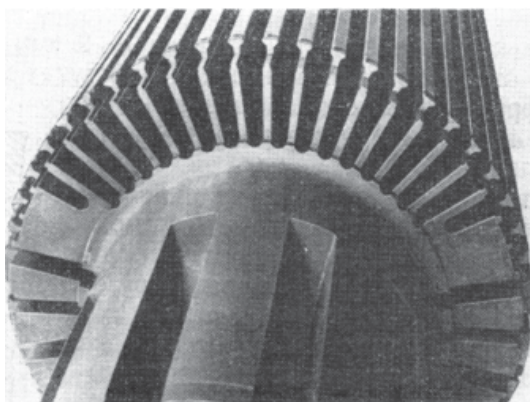


Fig. 7 Rotor of a synchronous turbogenerator

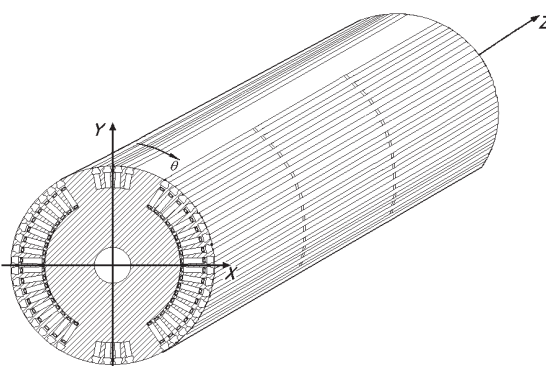


Fig. 8 Simplified model of turbogenerator rotor

Fig. 9 shows the calculated time evolution of the rotor surface temperature at the most heated point of the surface. The horizontal line indicates the permissible working temperature 160 °C of the turbogenerator insulation. The analysis of results allows estimating the admissible duration of

the turbogenerator operation at a line-to-line short circuit on two phases of the machine in various conditions of the rotor cooling (convective heat transfer to air and hydrogen cooling with various values of the surplus gas pressure  $p$ ). It can be seen that this duration depends strictly on the rotor gas cooling conditions and equals to about 1.02 s in the case of the most “weak” air cooling and 1.22 s in the case of the most “powerful” hydrogen cooling with the surplus pressure of the gas ( $p = 4$ ).

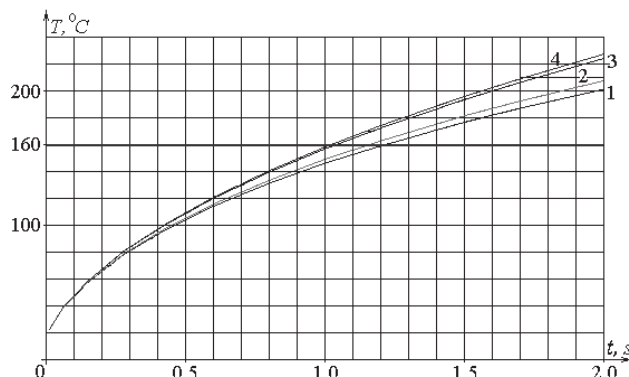


Fig. 9 Heating of rotor surface: 1–hydrogen cooling,  $p = 4$ ; 2–hydrogen cooling,  $p = 3$ ; 3–hydrogen cooling,  $p = 1$ ; 4 – air cooling

### B. Induction Heating of Large Steel Disks

This numerical example models a new technological process of induction heating of large steel disks using a common sinusoidal excitation [8]. The heated disks are used in hot plastic pressing of the container bottoms applied in chemical industry and in power engineering. This technology concerns the disks of diameters  $d \in \langle 0.5, 4 \rangle$  m and thickness of several millimeters. The induction heating of such disks with large ratios diameter versus thickness is characterized by technological difficulties connected with thermal deformations resulting from a non-uniform temperature distribution. These phenomena are observed as plastic deformations of the disk.

Fig. 10 presents the “inductor-disk” system under consideration including a heated steel disk and a planar copper inductor with 14 turns. The inductor voltage is 450 V at frequency of 8 kHz. Duration of induction heating is about 600 s.

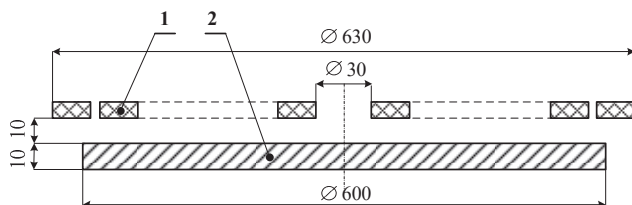


Fig. 10 Computer model of “inductor-disk” system: 1 – inductor, 2 – disk

The aim of the coupled magneto-thermal and elastic-plastic solution of the problem is to calculate the static deformed state of the disk. One can see that the disk radius can increase by 4

mm during the induction heating, but with axial displacement reaching only 1 mm (see Fig. 11). Besides, Fig. 11 presents the plastic and elastic zones distribution in the heated disk (plastic zones are shaded). In fact, the plastic zones occupy nearly the total volume of the heated disk. It means that the technological conditions of the induction heating were correctly chosen because the hot disk was ready for plastic forming.

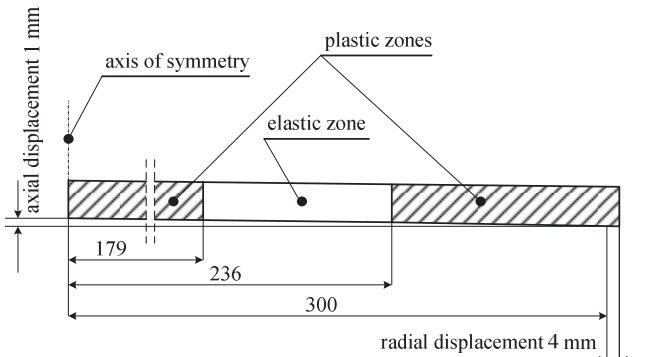


Fig. 11 Deformed state of the heated disk and plastic zones distribution

### C. Electromagnetic and Temperature Fields of a Household Induction Cooker

The typical design of an induction cooker and its inductor is presented in Fig. 12. In its turn, Fig. 13 shows examples of axisymmetrical computation models developed. The models include a copper inductor, a steel or aluminum pan with thin ferromagnetic layer, a ferrite core and non-conductive regions. The frequency of AC current in the inductor is 20-100 kHz.



Fig. 12 Design of an induction cooker and its inductor

The spatial distributions of electromagnetic and thermal fields are modelled by the EleFAnT2D computer code [13] in axisymmetrical formulation with corresponding boundary conditions. Examples of obtained distributions are presented in Fig. 14 ((a) – flux density distribution and (b) – pan's temperature field calculated).

### VI. CONCLUSION

The mathematical models and iterative numerical algorithms for finite element analysis of coupled magneto-thermo-mechanical behavior of electrical and electromechanical devices are described in detail. Peculiarities of numerical simulation of coupled multiphysical phenomena regarding various types of devices under consideration are discussed. Numerical results describing solution of actual problems of practical interest (industrial induction heaters, household induction cookers, turbogenerator rotors) are presented and analyzed.

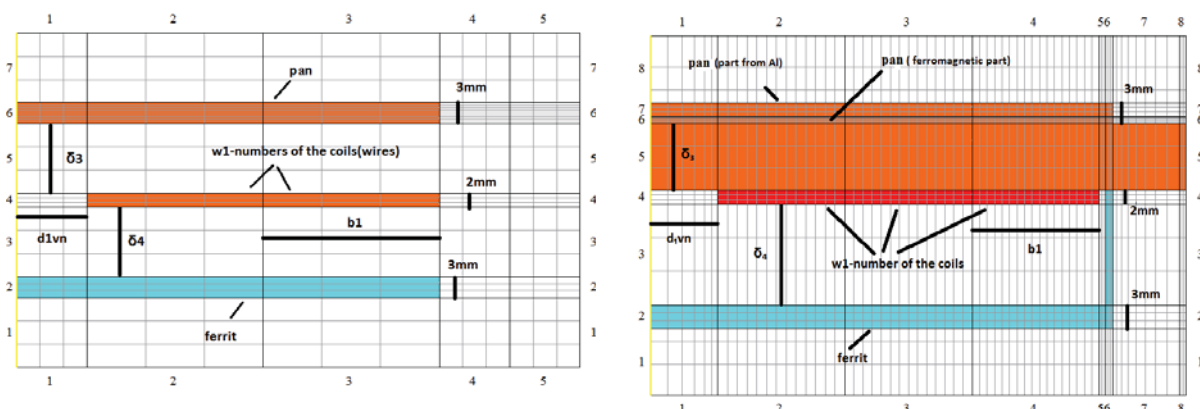


Fig. 13 Numerical models developed

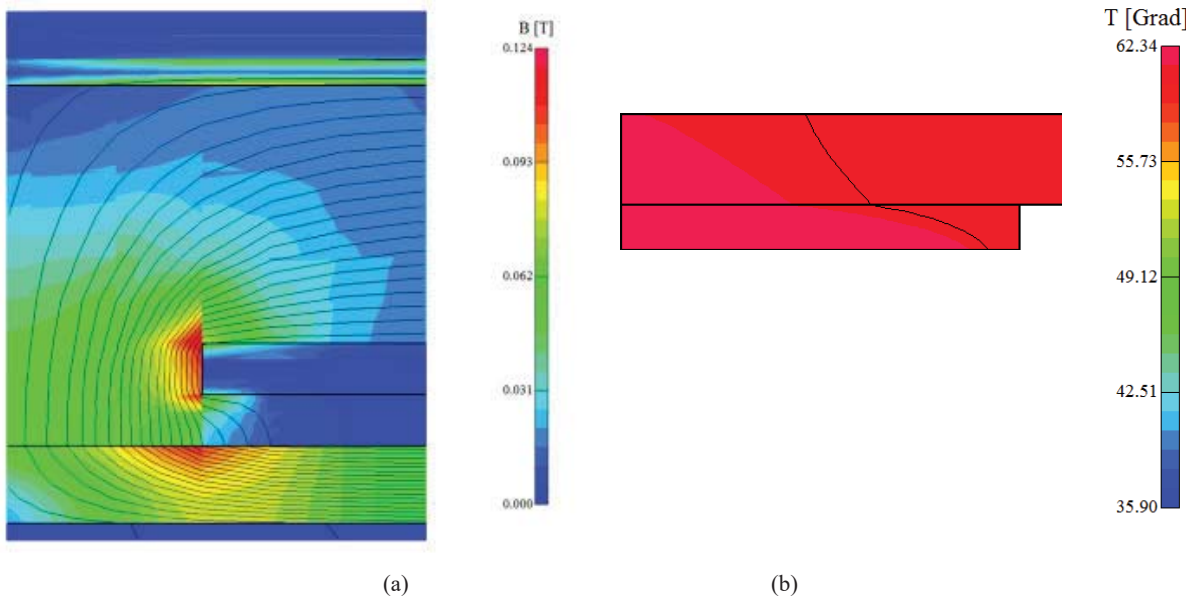


Fig. 14 Examples of obtained numerical results

#### REFERENCES

- [1] M. G. Pantelyat, "Multiphysical numerical analysis of electromagnetic devices: state-of-the-art and generalization," *Electrical Engineering & Electromechanics*, No. 3, pp. 29–35, 2013.
- [2] O. Bíró and K. Preis, "On the use of the magnetic vector potential in the finite element analysis of three-dimensional eddy currents," *IEEE Trans. Magn.*, vol. 25, No. 4, pp. 3145–3159, July 1989.
- [3] J. P. Holman, *Heat Transfer*, New York, NY: McGraw-Hill, 2002.
- [4] S. Timoshenko and J. N. Goodier, *Theory of Elasticity*, New York, NY: McGraw-Hill, 1951.
- [5] P. Sharifi and D. N. Yates, "Nonlinear thermo-elastic-plastic and creep analysis by the finite-element method", *AIAA Journal*, vol. 9, pp. 1210–1215, 1974.
- [6] I. Doležel, P. Karban, B. Ulrych, M. G. Pantelyat, Yu. I. Matyukhin, and P. P. Gontarowsky, "Numerical model of a thermoelastic actuator solved as a coupled contact problem", *COMPEL: The International Journal for Computation and Mathematics in Electrical and Electronic Engineering*, vol. 26, pp. 1063–1072, 2007.
- [7] M. G. Pantelyat and N. G. Shulzhenko, "On approximation for magnetization curves", in *Proc. 12<sup>th</sup> Int. IGTE Symp. Numerical Field Calculation in Electrical Engineering*, Graz, Austria, Sept. 2006, pp. 96–99.
- [8] J. Zgraja, M. G. Pantelyat, "Induction heating of large steel disks: coupled electromagnetic, thermal and mechanical simulation", *International Journal of Applied Electromagnetics and Mechanics*, vol. 10, pp. 303–313, 1999.
- [9] G. B. Kumbhar and S. V. Kulkarni, "Applications of coupled field formulations to electrical machinery", *COMPEL: The International Journal for Computation and Mathematics in Electrical and Electronic Engineering*, vol. 26, pp. 489–523, 2007.
- [10] S. C. Bhargava, "Negative-sequence currents, losses and temperature rise in the rotor of a turbogenerator during transient unbalanced operation", *Electric Machines and Power Systems*, vol. 8, pp. 155–168, 1983.
- [11] L. C. Meng, K. W. E. Cheng, and P. C. K. Luk, "Field analysis of an induction cooker with square 9-coil system by applying diverse exciting pattern", in *Proc. 6<sup>th</sup> IET Int. Conf. Power Electronics, Machines and Drives (PEMD 2012)*, Bristol, United Kingdom, March 2012, pp. 1-5.
- [12] R. Stancheva and I. Iatcheva, "Coupled electromagnetic and temperature field distribution in the end region of a large turbine generator under different operating conditions", in *Proc. 10<sup>th</sup> Int. IGTE Symp. Numerical Field Calculation in Electrical Engineering*, Graz, Austria, Sept. 2002, pp. 331–335.
- [13] <http://www.system-integration.at/system-integration/news/news-single/article//elefant-2d/>. Access date: 2016-04-20.